Simultaneously Controlled Directionality and Valency on a Water-Soluble Gold Nanoparticle Precursor for Aqueous-Phase Anisotropic Self-Assembly

ARTICLE *in* LANGMUIR · DECEMBER 2010

Impact Factor: 4.46 · DOI: 10.1021/la104114f · Source: PubMed

2 AUTHORS:

Jeong-Hwan Kim
Yokohama City University
43 PUBLICATIONS **426** CITATIONS
SEE PROFILE

Jin-Woo Kim
University of Arkansas
83 PUBLICATIONS **1,619** CITATIONS
SEE PROFILE

Langmuir
Letter
pubs.acs.org/Langmuir

Simultaneously Controlled Directionality and Valency on a Water-Soluble Gold Nanoparticle Precursor for Aqueous-Phase Anisotropic Self-Assembly

Jeong-Hwan Kim and Jin-Woo Kim*

Bio/Nano Technology Laboratory, Department of Biological and Agricultural Engineering and Institute for Nanoscale Materials Science and Engineering, University of Arkansas, Fayetteville, Arkansas 72701, United States

Received October 13, 2010. Revised Manuscript Received November 19, 2010

The anisotropic interaction of gold nanoparticles (AuNP's) into a highly accurate, scalable complex structure not only would aid practical nanoscale assembly but also would increase their utility in many applications, including electronics, optics, and biosensing. Particularly for biological purposes, here we demonstrate an aqueous-phase serial solid-phase monofunctionalization approach to synthesize water-soluble AuNP linkers that contain distinctive single or double diametric functionalities in a site-specific way. Using a mild, rapid, effective single-phase 1:1 ligand replacement reaction between mixed-ligand-protected AuNP precursors and ligand-group-attached silica gels, we successfully synthesized (1) two types of monofunctionalized (monof-) carboxyl- or amino-AuNP's with enhanced yield and accuracy and (2) heterobifunctionalized (bif-) AuNP's with one carboxyl and one amine end group at a discrete angle (∼160°). The controlled coupling chemistry in aqueous solution allowed the covalent bond-directed assembly of intentionally designed 1D dimers with monof-AuNP's and 2D rings with heterobif-AuNP's, confirming the highly functional as well as directional selectivity of the functionalized NPs. This study thus represents an important step toward active control over the design and assembly of bottom-up nanostructures with increased complexity and biocompatibility.

For the bottom-up hierarchical construction of complex nanoarchitectures, the programmed assembly of nanomaterials in a flexible manner is very important. The primary challenge in realizing this aim is to enable the anisotropic self-assembly of nanostructures with precise geometry, where previous work mainly focused on spherical nanoparticles (NPs) forming ordered monolayers.[1] However, there are no preferred complex orientations in such assemblies because of the spherical symmetry of the building blocks and the stoichiometric imbalance caused by their different reactivities.[2] Only a few results have been reported for controlled interfacing, with particular focus on a template-guided assembly format using biomolecular recognitive linkers such as DNA oligonucleotides.[3] However, the configurational basis of a specific interfacing (i.e., controlled number, location, orientation, and composition of linkers) is yet to be required in a fundamental building level to overcome the inherent isotropic nature in the molecular interactions on the nanoscale.

Recent advances led to the development of controlled asymmetric interfacing methodologies using solid-phase monofunctionalization of specific linkers on NP units.[4−6] The selection of proper solid supportive layers not only enabled individual NPs to influence the minimized chemical functional linkers at surfaces but also simultaneously permitted chemical reactions to be balanced by separation steps in the process. This opened the possibility to achieve discrete numbers of linkers in predetermined orientations on NPs and anisotropically self-assembled homo- or heterodimers or their radially sided structures.[4a,b] Also under a different scheme using the facial solid-phase functionalization method, a side-to-side assembly was proposed.[4c] Furthermore, to realize the single valency of an NP building block for more accurately assembled designs, efforts to minimize the loading level of functional linkers on monolayer-protected gold (Au) NPs were made on the basis of the ligand place exchange reaction, enabling more stable and efficient functionalization on the basis of the covalent bond chemistry.[5] Recently, our group has introduced an improved synthesis scheme, termed "sequential solid-phase functionalization",[6] demonstrated site-specific mono- and bifunctionalizations of building block interconnectors with defined directionality and functionality to yield improved control over diverse nanoscale structure assembly (i.e., 1D chains or 2D rings), and demonstrated the possibility of active control over the design and assembly of such hierarchical nanostructures.

However, the solid-phase monofunctionalization methods developed so far are inherently limited to the organic-solvent-based synthesis, which not only requires the use of a large quantity of solvent such as dichloromethane[5] but also yields water-immiscible NP products unsuitable to function within aqueous media for their biological and biomedical applications. Furthermore, the conventional ligand-exchange strategy typically uses thiolated-ligand-capped AuNP precursors and primarily involves strong, irreversible covalent binding, which leads to lowering the fraction of transferrable ligands.[7] As a result, the scope of the organic-phase

*Corresponding author. E-mail: jwkim@uark.edu. Tel: +1-479-575-2351. Fax: +1-479-575-2846.

(1) Glotzer, S. C.; Solomon, M. J. *Nat. Mater.* **2007**, *6*, 557–562.
(2) (a) Akcora, P.; Liu, H.; Kumar, S. K.; Moll, J.; Li, Y.; Benicewicz, B. C.; Schadler, L. S.; Acehan, D.; Panagiotopoulos, A. Z.; Pryamitsyn, V.; Ganesan, V.; Ilavsky, J.; Thiyagarajan, P.; Colby, R. H.; Douglas, J. F. *Nat. Mater.* **2009**, *8*, 354–359. (b) Barth, J. V.; Costantini, G.; Kern, K. *Nature* **2005**, *437*, 671–679.
(3) Becerril, H. A.; Woolley, A. T. *Chem. Soc. Rev.* **2009**, *38*, 329–337.
(4) (a) Xu, X.; Rosi, N. L.; Wang, Y.; Huo, F.; Mirkin, C. A. *J. Am. Chem. Soc.* **2006**, *128*, 9286–9287. (b) Sardar, R.; Heap, T. B.; Shumaker-Parry, J. S. *J. Am. Chem. Soc.* **2007**, *129*, 5356. (c) Sardar, R.; Shumaker-Parry, J. S. *Nano Lett.* **2008**, *8*, 731–737.
(5) (a) Worden, J. G.; Dai, Q.; Shaffer, A.; Huo, Q. *Chem. Mater.* **2004**, *16*, 3746–3755. (b) Sung, K.-M.; Mosley, D. W.; Peelle, B. R.; Zhang, S.; Jacobson, J. M. *J. Am. Chem. Soc.* **2004**, *126*, 5064. (c) Liu, X.; Worden, J. G.; Dai, Q.; Zou, J.; Wang, J.; Huo, Q. *Small* **2006**, *2*, 1126–1129.
(6) Kim, J.-H.; Kim, J.-W. *Langmuir* **2008**, *24*, 5667–5671.
(7) (a) Gittins, D. I.; Caruso, F. *Angew. Chem., Int. Ed.* **2001**, *40*, 3001–3004. (b) Zanchet, D.; Micheel, C. M.; Parak, W. J.; Gerion, D.; Alivisatos, A. P. *Nano Lett.* **2001**, *1*, 32. (c) Warner, M. G.; Reed, S. M.; Hutchison, J. E. *Chem. Mater.* **2000**, *12*, 3316–3320. (d) Gandubert, V.; Lennox, R. B. *Langmuir* **2005**, *21*, 6532–6539.

Scheme 1. Sequential Solid-Phase Synthesis of Water-Soluble MUA-Monofunctionalized, AUT-Monofunctionalized, and MUA-AUT-Heterobifunctionalized Gold Nanoparticles[a]

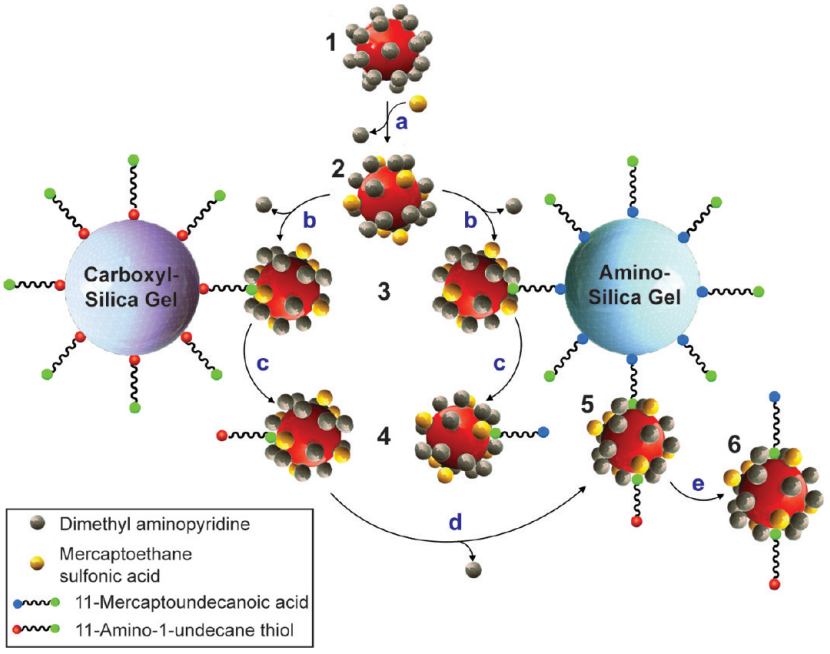

[a] Reagents and conditions: (a) 43 μM MESA, 4 h, 25 °C. (b) H_2O, 1 h, 25 °C. (c) 0.5% TFA, CH_3OH. (d) H_2O, 1 h, 25 °C. (e) 0.5% TFA, CH_3OH.

ligand exchange is restricted, making it difficult to achieve multistep ligand modifications to realize heterogeneous valency with multiple functional groups in defined directionality and functionality. Additionally, it is very difficult to control the size and monodispersity of such organic-phase NPs in aqueous environments, usually requiring laborious size-sorting steps such as gel permeation chromatography.[7] The NP's monodispersity is very important for the effective, accurate self-assembly of nanostructures with minimal errors because polydispersity is one of the main sources of errors in the nanoscale assembly process.[8a] The use of water-soluble monolayers on the NP precursors in the initial stage of the ligand-exchange reaction may enable us to overcome the significant hurdles in the organic phase reaction and to produce final products that are readily suitable for biological applications, which commonly occur in biologically relevant aqueous solutions. Recently, one-step synthesis methods for water-soluble monodisperse AuNP's with appropriate stabilizing ligands, such as 4-(dimethylamino)pyridine (DMAP)[7a] or bis-(*p*-sulfonatophenyl)phenylphosphine dipotassium salt (BSPP),[7b] were reported. These NPs were demonstrated to be highly monodisperse in aqueous solution with controllable size tunability and compatibility with biological manipulations owing to their biologically amenable surface capping or passivating ligands.[8]

We designed an aqueous-phase ligand replacement strategy to produce water-soluble, biocompatible AuNP's with defined locations, orientations, and compositions of functional ligand groups. Our technology was developed by synergistically integrating the water-soluble AuNP precursors[7] and our previously demonstrated sequential solid-phase functionalization approach[6] with necessary modifications and optimizations. We hypothesized that not only the ligands with amine[7a] or phosphine[7b] headgroups (i.e., DMAP or BSPP) may serve as suitable protective layers surrounding hydrophobic AuNP cores to render high solubility and monodispersity in water but also the relatively weaker interactions between amine[7a] or phosphine[7b] and gold (as compared to those between thiol and gold) may allow more efficient displacement with incoming ligands with thiol headgroups during the solid-phase ligand-exchange reaction. The intent of this investigation was to validate the hypothesis by establishing the first general aqueous-phase approach to synthesize water-soluble monofunctionalized (monof-) as well as bifunctionalized (bif-) NPs in a site-specific manner by loading a single functional group at a time. The aqueous-phase anisotropic or symmetric functionalizations were confirmed by demonstrating that the resultant site-specific construction units yield intentionally directed self-assembled 1D and 2D nanostructures (i.e., 1D dimers and 2D rings) in an aqueous medium (i.e., water) with greater control and accuracy.

The developed synthesis protocol is shown in Scheme 1. The AuNP's protected by a monolayer of DMAP (DMAP-AuNP, dAuNP)[7a] **1** were used as a robust model of water-soluble NP precursors. First, the dAuNP was subjected to controlled ligand exchange with mercaptoethane sulfonic acid (MESA) to synthesize water-soluble AuNP's with stabilizing layers mixed with DMAP and MESA (DMAP-AuNP-MESA, dmAuNP) **2** using our modified method on the basis of ref 7c. Such a modification was necessary to compensate for the chemical instability of DMAP under acidic conditions (i.e., pH < 5),[7d] which is required for the cleavage steps during the solid-phase ligand-exchange reaction as well as its physical instability during the centrifugation steps, which is required for the product separations. Briefly, 1 mg/mL of dAuNP's in water/toluene (10:1, v/v) was mixed with varying concentrations of MESA. The reaction mixture was incubated for 4 h at 25 °C, and the final pH was ~5. At this pH, the endocyclic amine group of the outgoing DMAP during the ligand-exchange reaction would be mostly protonated;[7d] hence, they were unable to bind back to the gold surface in the presence of MESA. After the ligand-exchange reaction, the resultant dmAuNP's were separated from dissociated DMAP and remaining free MESA ligands by a simple phase transfer between water and organic

(8) (a) Pileni, M.-P. *Nanocrystals Forming Mesoscopic Structures*; Wiley-VCH: Weinheim, Germany, 2005. (b) Roduner, E. *Nanoscopic Materials: Size-Dependent Phenomena*; RSC Publishing: Cambridge, U.K., 2009.

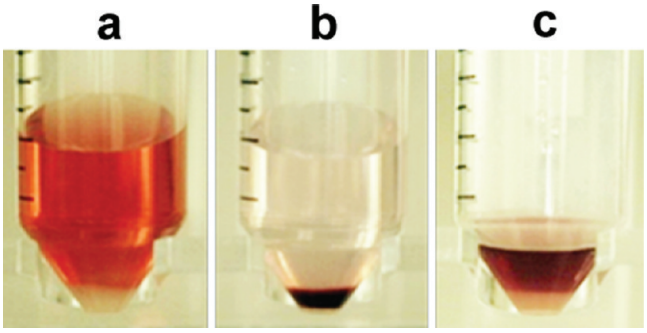

Figure 1. Reaction solutions during the first sequence of the aqueous-phase ligand-exchange reaction. Bifunctionalization was achieved by repeating the anisotropic aqueous-phase functionalization technique with monofunctionalized dmAuNP. (a) Before the ligand-exchange reaction right after mixing dmAuNP and silica gels. (b) After the ligand-exchange reaction. (c) After cleavage with 0.5% TFA to yield functionalized dmAuNP.

solvents with the addition of dichloromethane (DCM) (20 mL), followed by methanol (20 mL). Such a simple and convenient phase-transfer separation was possible owing to the unique water-soluble characteristics of dAuNP's[7a] as well as dmAuNP's after ligand-exchange reactions. The DMAP and MESA were preferably partitioned into the organic phase, leaving the dmAuNP's in the water phase. After removal of the organic layer with DMAP and MESA, the remaining solvent layer was thoroughly evaporated under flowing N_2. The 1/0.07 molar ratio of DMAP/MESA (i.e., 1 mg/mL of dAuNP's with 43 μM of MESA, assuming the concentration of DMAP is 0.6 mM in 1 mg/mL of dAuNP's[7d]) was shown to be optimal for providing the necessary stability as well as aqueous solubility (as exemplified in Figure 1), which are critical to implementing the designed solid-phase ligand-exchange reaction in aqueous solution. (Details of the results of the optimization experiments are in Supporting Information). The resultant dmAuNP with the mixed monolayer (i.e., AuNP comodified with weak DMAP and strong MESA ligands) had a net negative charge, characterized by gel electrophoresis analyses (Figure S1, inset, Supporting Information) owing to the major influence from the sulfonic acid groups of MESA. In contrast, dAuNP with the DMAP monolayer had a net neutral charge in gel electrophoresis. The effective migration of the NP products in the gel demonstrates their high water solubility, and the narrow bands imply their outstanding monodispersity in water. The anisotropic patterning procedure began with the synthesis of monof-dmAuNP (R-Au or R′-AuNP) from dmAuNP according to our modified silica-gel-based method from the earlier protocols (Figure 1).[5c,6] Briefly, dual types of microspheres, amino- (*N*-) or carboxyl- (*C*-) silica gels (SGs) (0.03 g/mL) in DCM/methanol (1:1, v/v), were used, and both SGs were electrostatically loaded with bifunctionalized amphiphilic linkers (8.3 μM) (i.e., 11-mercaptoundecanoic acid ($(HO_2C(CH_2)_{10}SH$, MUA, R) for N-SGs and 11-amino-1-undecanethiol ($H_2N(CH_2)_{10}SH$, AUT, R′) for C-SGs). The ligand place exchange reaction occurred by replacing DMAP on AuNP with the amphiphilic linker on SGs (i.e., MUA or AUT) **3** for 1 h at 25 °C, followed by washing with a copious amount of water, cleavage with trifluoroacetic acid (TFA) in methanol (~0.5%), and purification steps with petroleum ether to yield monof-dmAuNP **4**. After monofunctionalization, the opposite point of the ligand on the monof-dmAuNP (i.e., R-AuNP) was subjected to another ligand exchange on the R′-modified SGs for bifunctionalization **5**. The final products (i.e., bif-dmAuNP, R-AuNP-R′, and **6**) were acquired after the washing, cleaving,

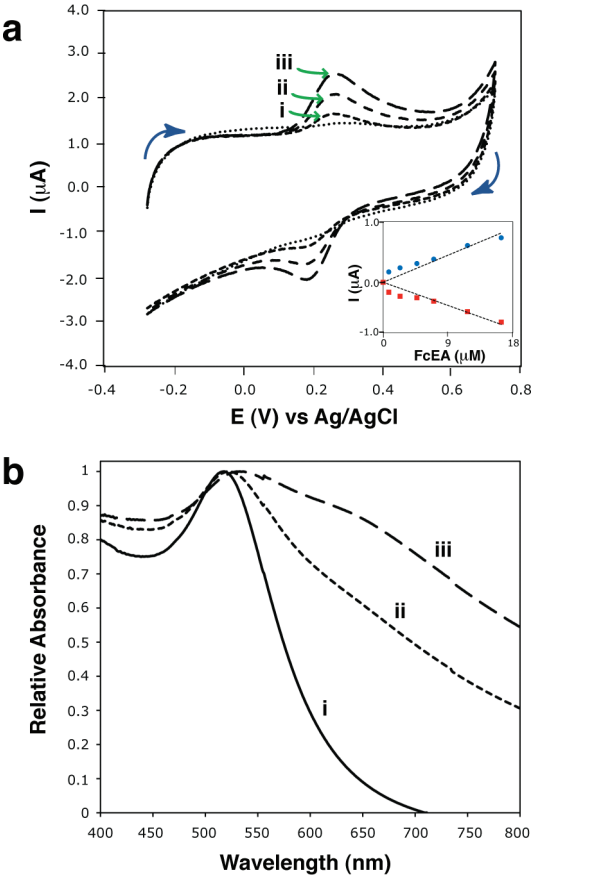

Figure 2. (a) Cyclic voltammograms of FcEA-conjugated AuNP's. (i) FcEA-conjugated dmAuNP's (control), (ii) FcEA-conjugated monofunctionalized dmAuNP's, and (iii) FcEA-conjugated homobifunctionalized dmAuNP's. The inset is a calibration plot of FcEA's. The measured separation potential (ΔE, p = X) at all scan rates was 0.1 V and was correlated with a characteristic value of Fc in aqueous systems. (b) UV/vis/NIR absorption spectra of the dmAuNP's before and after the coupling reactions. (i) Free dmAuNP's, (ii) directional assembly products of monofunctionalized dmAuNP's (1D dimers), and (iii) directional assembly products of heterobifunctionalized dmAuNP's (2D rings). Each datum point was normalized on the maximal absorption in the wavelength range of 400 to 800 nm for the plasmon responses of each product.

and purification steps. (Details of the experimental procedures in the ligand place exchange reactions are in Supporting Information.) For the purified products, cyclic voltammetry (CV) was used to assess their functionality. Ultraviolet/visible/near-infrared (UV/vis/NIR) spectroscopy was used to evaluate their functionality and yield estimations. Coupling reactions of the final products were designed to evaluate the directionality as well as the functionality of the functional groups on the AuNP's. The coupling reaction products were examined by atomic force microscopy (AFM) in tapping mode in air and transmission electron microscopy (TEM). (Details of the experimental procedures and image analyses are in the Supporting Information.)

Our aqueous-phase functionalization method was shown to require much less ligand exchange reaction time and milder conditions for the cleavage steps compared to the previous organic-phase thiol-to-thiol replacement reactions.[5,6] The aqueous-phase exchange reaction was completed within 1 h (cf. 8−12 h for the organic-phase reactions[5]). The weaker adsorption affinity of the amino headgroup of DMAP on the surface of AuNP (compared to the thiol headgroup) allowed such a rapid, effective exchange

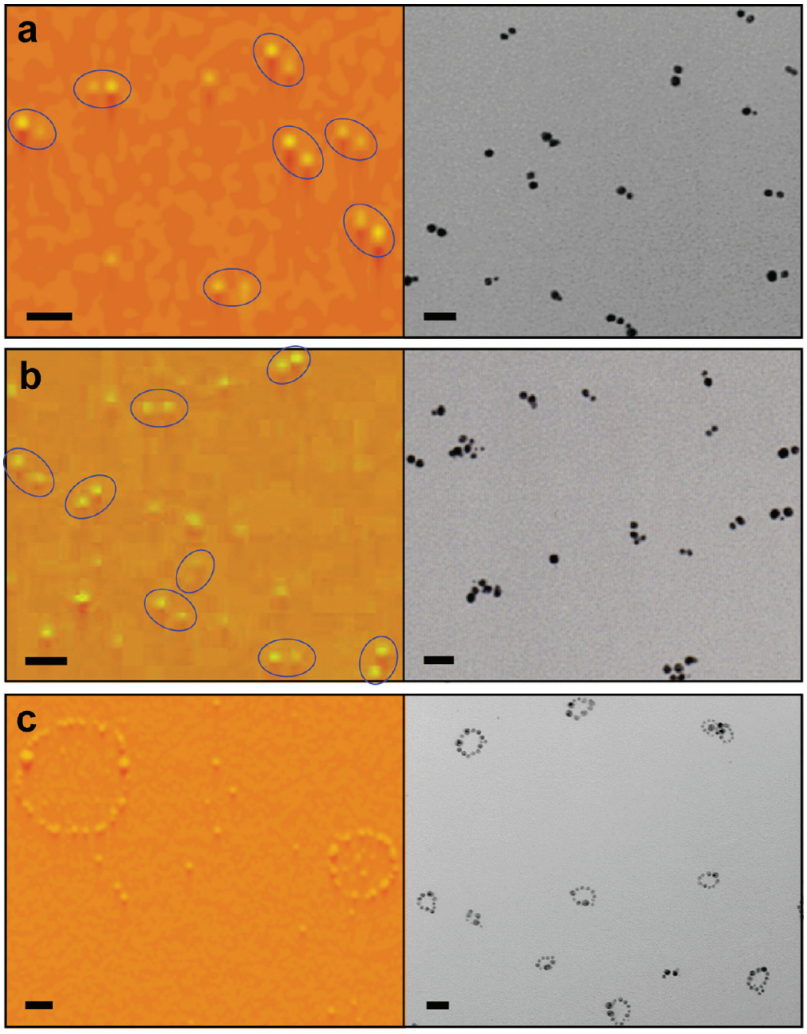

Figure 3. Phase AFM (left) and TEM (right) images of directional assembly products of (a) MUA-monofunctionalized dmAuNP's (1D dimers), (b) AUT-monofunctionalized dmAuNP's (1D dimers), and (c) MUA-AUT heterobifunctionalized dmAuNP's (2D rings). (a, b) Circles in AFM images indicate dimers. The scale bar is 10 nm.

reaction, proving the aforementioned underlying hypothesis of our technology. After rinsing off any unbound NPs, the NPs attached to the SGs were immediately released using ~0.5% TFA in methanol, which is much milder than for earlier reports using highly concentrated acidic cocktails (20^{5c}–$60^{5a,b}$%). The non-covalently and electrostatically bound functional linkers (i.e., R or R′) on the charged solid supports (i.e., N- or C-SGs) were attributed to such an effective cleavage even under much milder conditions. These highly efficient and mild exchange and cleavage reactions contributed to less loss (< 35%) of the functionalized products, resulting in a higher production yield (> 65%) compared to that of the previous organic-phase reactions.[5,6] Finally, dmAuNP with the mixed monolayer of DMAP and MESA was very stable during the course of the entire functionalization reaction and showed high water solubility even after the ligand-exchange reactions.

The functionalization efficacy was assessed by analyzing the functionalized NP products with CV after coupling their carboxyl ends with a redox probe, ferrocene ethylamine (FcEA) (Figure 2a). FcEA coupling was done at the end of each functionalization step. To alleviate the difficulty in separating the unbound excess FcEA in the aqueous phase, the purification (i.e., washing off unbound FcEA) and CV analyses were done after the attachment of the functionalized dmAuNP products coupled with FcEA to the N-SGs (i.e., after another ligand exchange). The CV analyses showed well-resolved, reversible redox signals for the FcEA-coupled dmAuNP (Figure 2a,i). The signal intensities increased proportionally as the number of Fc moieties conjugated to the functional linkers (i.e., R) on dmAuNP increased (Figure 2a,ii, iii). On the basis of the FcEA calibration curve (Figure 2a, inset), the estimated concentrations of FcEA-conjugated R-AuNP and R-AuNP-R were 4.2 and 9.0 μM, respectively. This implies that bif-dmAuNP has approximately twice as many R groups per unit mass as monof-dmAuNP, indicating that our aqueous-phase functionalization method worked as designed and allowed control over the chemical valency of the ligands on the AuNP's. This demonstrates that the aqueous-phase functionalization procedure is as efficient as (if not more efficient than) the organic-phase reaction.[6] Again, the functionalized products were very soluble in water and very stable, showing minimal signs of aggregation under ambient conditions for at least 3 months.

To verify the directional functionality of linkers on NPs, we utilized two different coupling modes: (1) a coupling reaction with glutaraldehyde (GA) for homodimers with R-AuNP and (2) a 1-ethyl-3-(3-dimethylaminopropyl)carbodiimide hydrochloride/*n*-hydroxysulfosuccinimide (EDC/sulfo-NHS) coupling reaction to produce heterodimers between R-AuNP and R′-AuNP products as well as 2D structures with R-AuNP-R′. (Details of the

experimental procedures are in the Supporting Information.) First, after the coupling reactions, the surface plasmon resonance (SPR) responses of the coupled products were assessed using UV/vis/NIR spectroscopy (Figure 2b). As similarly observed in our previous study,[6] the SPR peaks of the coupled products were red shifted and broadened with appreciably strong absorbance toward the NIR from the characteristic peak of dmAuNP at 515 nm. This implies the possibility of tuning the NPs' optical properties via their controlled assembly. This unique optical property would be very useful for a variety of biological and biomedical applications, including minimally invasive and highly target-specific diagnostics and therapies based upon NIR laser-induced thermal and acoustic responses of the NPs or NP complexes.[9] Next, the structural characterization of the coupled products was carried out using AFM and TEM to confirm their functionality, geometry, coupling yield, and dispersity. Estimated with AFM in tapping mode in air and TEM, the dmAuNP sample was well dispersed and its average size was found to be 2.77 ± 0.92 nm (AFM) and 2.65 ± 0.45 nm (TEM) (Figure 3 and Tables S1 and S3, Supporting Information) (i.e., estimated from over 100 different particles). The dominant presence of dimeric species was observed after both EDC/sulfo-NHS and GA coupling reactions with monof-dmAuNP (Figure 3a,b). The estimated yields of the heterodimers (i.e., AuNP-R-R′-AuNP by EDC/sulfo-NHS coupling) and homodimers (i.e., AuNP-R-R-AuNP by GA coupling) were 70 and 81% (AFM) and 71 and 70% (TEM), respectively (Tables S2 and S3, Supporting Information). This is comparable to the results in the organic-phase reaction.[6] On the basis of high-resolution AFM, the interparticle spacings of the dimeric NPs were 1.71 ± 0.25 nm for the heterodimers and 1.73 ± 0.22 nm for the homodimers; from the TEM images, they were 1.70 ± 0.212 nm and 1.74 ± 0.103 nm respectively (Tables S2 and S3, Supporting Information). This corresponds well to actual linker lengths of ca. 2.19 nm (i.e., MUA-EDA-AUT) and 2.34 nm (i.e., MUA-GA-MUA). When assessing the coupled products of the heterobif-dmAuNP with AFM and TEM, 2D oligomeric rings (Figure 3c) were assembled. The ring formation with R-AuNP-R′ with amine and carboxyl groups at opposite ends indicates the meta-coordination of the functional ligands from the NP center. Estimated with AFM and TEM analyses (Tables S2 and S3, Supporting Information), the interparticle spacings of the 2D ring were 1.85 ± 1.24 nm (i.e., estimated from about 288 particles) and 1.74 ± 0.62 nm (i.e., estimated from about 100 particles), respectively. The average angle between three particles in the ring string was $158.6 \pm 16.79°$ and the yield was ~47% from AFM analysis; the average angle between three particles in the ring string was $150.8 \pm 19.57°$ and the yield was ~46% from TEM analysis. The results are comparable to those in the organic phase in our previous study.[6] Further studies are still required to optimize the aqueous-phase ligand-exchange reaction as well as to expand the functionality and directionality. However, this study demonstrates its high potential to synthesize anisotropically or symmetrically functionalized NPs not only with active control over the functionality and directionality of the functional groups but also with high water solubility and stability, which are very desirable for their biological and biomedical applications.

In summary, an aqueous-phase ligand-exchange methodology was developed in this study to produce water-soluble NPs anisotropically or symmetrically functionalized with functional ligands in a site-specific manner. The method was designed on the basis of the chemistry of the water-soluble AuNP's (i.e., dAuNP's) and the previously reported sequential solid-phase functionalization approach in the organic phase[6] with proper modifications. In particular, the successful modification of the protective layer of the stabilizing ligands on the water-soluble AuNP's (i.e., from the DMAP layer to the mixed layer with DMAP and MESA) enabled us to overcome the inherent instability (in particular, under acidic conditions) of the original dAuNP and to implement successfully the designed water-phase functionalization procedure. Our developed aqueous-phase approach allowed highly controlled functionalizations for synthesizing anisotropically monofunctionalized and bifunctionalized NP linkers with high yield and accuracy, which is comparable to those in the previous organic-phase reaction.[6] Compared to the organic-phase reactions, however, the aqueous ligand-exchange reaction proceeded much more rapidly and under milder conditions, making our developed protocol more efficient and environmentally friendly. Also of note is the NPs' high stability and solubility in water, which cannot be achieved in organic-solvent-based synthesis. Such high water compatibility presents great promise for their practical applications in biological and biomedical systems, including their bioinspired self-assembly applications for addressable bioprocessors, site-specific cancer therapy, and pinpoint-targeted drug/gene delivery systems.

Acknowledgment. This work was supported in part by the National Science Foundation (NSF) (awards CMMI-0709121 and CCF-0523858) and the Arkansas Biosciences Institute. We thank Russell Deaton for invaluable discussions with respect to this study.

Supporting Information Available: Experimental details of the preparation of functionalized AuNP's and analytical procedures. Functional characterizations of functionalized AuNP's. This material is available free of charge via the Internet at http://pubs.acs.org.

(9) (a) Kim, J.-W.; Galanzha, E. I.; Shashkov, E. V.; Moon, H.-M.; Zharov, V. P. *Nat. Nanotechnol.* **2009**, *4*, 688–694. (b) Galanzha, E. I.; Shashkov, E. V.; Kelly, T.; Kim, J.-W.; Yang, L.; Zharov, V. P. *Nat. Nanotechnol.* **2009**, *4*, 855–860. (c) Galanzha, E. I.; Kokoska, M. S.; Shashkov, E. V.; Kim, J.-W.; Tuchin, V. V.; Zharov, V. P. *J. Biophoton.* **2009**, *2*, 528–539. (d) Galanzha, E. I.; Kim, J.-W.; Zharov, V. P. *J. Biophoton.* **2009**, *2*, 725–735. (e) Kim, J.-W; Galanzha, E. I.; Shashkov, E. V.; Kotagiri, N.; Zharov, V. P. *Lasers Surg. Med.* **2007**, *39*, 622–634. (f) Zharov, V. P.; Galanzha, E. I.; Shashkov, E. V.; Kim, J.-W.; Khlebtsov, N. G.; Tuchin, V. V. *J. Biomed. Opt.* **2007**, *12*, 051503. (g) Zharov, V. P.; Kim, J.-W.; Curiel, D. T.; Everts, M. *Nanomedicine* **2005**, *1*, 326–345.